Strong field tunnel ionization by real-valued classical trajectories
Spanner, Michael

National Research Council Canada   Conseil national de recherches Canada

Canada

Strong Field Tunnel Ionization by Real-Valued Classical Trajectories

Michael Spanner

Department of Physics, University of Waterloo, Ontario, N2L 3G1 Canada
and Steacie Institute for Molecular Sciences, NRC Canada, 100 Sussex Drive, Ottawa, Ontario, K1A 0R6 Canada

Strong field tunnel ionization of an atom is considered from the point of view of semiclassical initial value representation methods which are based on real-valued classical trajectories alone. While the straightforward application of such propagators fails to give an accurate description of tunnel ionization in one dimension, incorporating the semiclassical propagator into *S*-matrix techniques standard in strong field physics leads to a more accurate method which recovers the tunneling dynamics. From the point of view of strong field physics, this procedure offers a method of incorporating core effects into the standard strong field approximation. In two dimensions, both the standard and the new semiclassical propagators are shown to give equally accurate results at sufficiently short times, but the new method exhibits much better scaling of the convergence rate with increasing dimensionality.

The problem of tunneling by real-valued classical trajectories alone has had an interesting history in recent years. It was suggested [1] that these trajectories were adequate to describe the tunneling process since any wave packet incident on a barrier will always contain some classically allowed real-valued trajectories with above-barrier energies. However, Ref. [2] demonstrated that for 1D problems with realistic barrier shapes (i.e., non-parabolic) the contribution of these classically allowed trajectories is not enough and the inclusion of classically forbidden paths is required to recover the correct tunneling probability. The present Letter outlines a new approach, built on the semiclassical initial value representation (SC-IVR) methodology [3] and the strong field formalism [4], which attempts to capture tunneling effects using only classically allowed trajectories. This new approach reproduces exactly the tunnel ionization described within the quantum mechanical strong field approximation (SFA) [4] when similar assumptions are applied to the semiclassical propagator. SFA is a standard and successful approach used to treat tunnel ionization in laser fields. Furthermore, the new approach also includes effects of the atomic core, usually neglected in SFA. Thus, it should indeed give a relatively accurate description of tunneling.

From the point of view of SC-IVR, the present work complements alternate procedures for incorporating tunneling effects into these methods [5,6]. It continues recent work [7] to extend SC-IVR methods, which have mostly been restricted to problems of field free and low-field molecular dynamics [3], to the area of strong field physics. Furthermore, the results presented below suggest that even the standard SC-IVR can be adequate to simulate short-time multidimensional atomic tunneling. However, the new procedure exhibits favorable scaling of the convergence rate with increasing dimensionality when compared to the standard SC-IVR. From the point of view of

strong field physics, this Letter offers a new method of incorporating core effects into the strong field approximation [4].

SC-IVR methods begin by writing the wave function at time t as an integral over the initial wave function Ψ_i

$$\Psi(x, t) = \int dx' K(x, x', t)\Psi_i(x'), \qquad (1)$$

where $K(x, x', t)$ is the full quantum propagator

$$K(x, x', t) = \langle x|e^{-i\hat{H}t}|x'\rangle. \qquad (2)$$

Atomic units are used throughout. Using the Herman-Kluk (HK) semiclassical IVR [8,9], the quantum propagator is replaced with the semiclassical approximation given by

$$K^{HK}(x, x', t) = (2\pi)^{-1} \iint dp \, dq \, C(p, q, t)$$
$$\times e^{iS(p,q,t)}\langle x|p_t q_t \gamma_1\rangle\langle pq\gamma_2|x'\rangle, \qquad (3)$$

where (p, q) represent the initial coordinates of classical trajectories, (p_t, q_t) are the final coordinates of these trajectories propagated via Hamilton's equations to time t, $S(p, q, t)$ is the classical action along these trajectories, and $|pq\gamma\rangle$ are coherent state (CS) wave packets with average position q and momentum p

$$\langle x|pq\gamma\rangle = \left(\frac{2\gamma}{\pi}\right)^{1/4}\exp[-\gamma(x-q)^2 + ip(x-q)]. \qquad (4)$$

The specific form of the prefactor $C(p, q, t)$ as well as the action and the necessary classical equations of motion are in [9]. The SC-IVR wave function at time t can then be written as

$$\Psi^{HK}(x, t) = (2\pi)^{-1}\iint dp \, dq \, C(p, q, t)e^{iS(p,q,t)}$$
$$\times \langle x|p_t q_t \gamma_1\rangle\langle pq\gamma_2|\Psi_i\rangle. \qquad (5)$$

This integral is typically evaluated using Monte Carlo integration with a sampling function $|\langle pq\gamma_2|\Psi_i\rangle|$.

The HK propagator (3) can be thought of as an expansion in an overcomplete set of CS wave packets whose centers follow classical trajectories up to time t at which point the CS wave packets are summed up to reconstruct the propagator. The original Herman-Kluk propagator sets $\gamma_1 = \gamma_2$. Here these Gaussian widths are allowed to differ to better reflect the characteristic sizes of the initial and final wave functions which, in some cases, leads to more accurate results as compared to the original Herman-Kluk expression. Overlaps for changing from the $|p_t q_t \gamma_2\rangle$ to the $|p_t q_t \gamma_1\rangle$ basis are included in $C(p, q, t)$.

Consider now a system with Hamiltonian $\hat{H} = \hat{H}_0 + \hat{V}$ where $\hat{H}_0$ is the field-free Hamiltonian and $\hat{V}$ is the interaction with a strong field. Direct substitution into the Schrödinger equation shows that the exact solution can be written as

$$\Psi(x, t) = -i \int_{t_0}^{t} dt' \langle x|e^{-i\hat{H}(t-t')}\hat{V}e^{-iH_0(t'-t_0)}|\Phi_0\rangle$$
$$+ \langle x|e^{-i\hat{H}_0 t}|\Phi_0\rangle, \qquad (6)$$

where $|\Phi_0\rangle$ is the initial state. The S-matrix amplitudes $S_{f0}(t \leftarrow t_0) = \langle \Phi_f|\Psi(t)\rangle$ which can be derived from Eq. (6) form the basis of many approximate strong field theories [4]. Equation (6) is referred to herein as the strong field S-matrix wave function.

The physical picture offered by this formalism is then as follows. The wave function propagates field-free until some time t'. It then receives a kick $\hat{V}$ from the field and propagates the remaining time $(t - t')$ in the field. The integral indicates that the wave function can be "kicked into the field" at any time and these contributions must all be summed.

Semiclassical evaluation of Eq. (6) for some initial eigenstate simply replaces the field-free propagator with the phase evolution of the eigenstate energy $e^{-i\hat{H}_0(t'-t_0)} = e^{-iE_0(t'-t_0)}$ and the full propagator $e^{-i\hat{H}(t-t')}$ with the semiclassical propagator to get

$$\Psi^{SF}(x, t) = -\frac{i}{2\pi} \int_{t_0}^{t} dt' \iint dp dq\, C(p, q, t, t') e^{iS(p,q,t,t')}$$
$$\times e^{-iE_0(t'-t_0)} \langle x|p_t q_t \gamma_1\rangle\langle pq\gamma_2|\hat{V}|\Phi_0\rangle$$
$$+ \langle x|e^{-iE_0 t}|\Phi_0\rangle \qquad (7)$$

where the classical paths are calculated using the full Hamiltonian H, start at time t', and propagate until the final time t. The semiclassical prefactor as well as the action then become formally dependent on t' (the "kick" time) and t (the observation time). This equation is referred to herein as the semiclassical strong field S-matrix approximation (SSF). The following analysis will be concerned with evaluating Eq. (7) numerically as is standard for semiclassical IVR methods. Brabec and co-workers [10], who have independently arrived at Eq. (7), are

currently approaching the solution by analytical means more common in the strong field literature.

Tunneling effects, as calculated using the HK expression Eq. (5), rely on the contribution from classical trajectories with above-barrier energy. However, since these trajectories are not bound to the core, they will eventually all propagate away leaving no continuous tunneling amplitude. Equation (7), on the other hand, allows for trajectories with above-barrier energy to originate near the core at any moment of time due to the integral over t' and hence this expression is expected to be better than the HK expression in that it contains a mechanism to generate a continuous tunneling amplitude. Furthermore, as will be shown below, it is Eq. (7) which reduces to the strong field approximation when similar assumptions are applied to the semiclassical propagator.

The first system used to test the SSF approximation is a 1D softcore atom in a constant electric field

$$H = H_0 - \mathcal{E}_0 x = \frac{1}{2} p^2 - \frac{1}{\sqrt{x^2 + a^2}} - \mathcal{E}_0 x, \qquad (8)$$

with $a = 1$. The potential $-\mathcal{E}_0 x$ was truncated at $x = 40$ a.u. to a constant $V = -40\mathcal{E}_0$ to prevent the wave function from accelerating rapidly away from the core. The initial wave function was the ground state (energy $E_0 = -0.670$ a.u.) approximated with a CS ($\gamma = 0.215$, $q = p = 0$). The field strength was $\mathcal{E}_0 = 0.075$ a.u.

Equation (7) could be evaluated directly using Monte Carlo integration for both the time and phase space integrals. However, since $\hat{V}$ is constant in time, further simplifications are possible. Specifically, all the classical dynamics [and hence $S(p, q, t, t')$ and $C(p, q, t, t')$] which are in general dependent on both t (the observation time) and t' (the kick time) become dependent on $t - t'$ only (the propagation time after the kick). Therefore, for any initial phase point (q, p), all possible kick times t' will lead to the identical classical dynamics and will vary only by the particular propagation time $t - t'$ needed to reach the observation time t. The time integral in Eq. (7) can then be summed up by propagating each initial phase point for the full time interval and summing up the contribution at each time point along the trajectories as opposed to propagating new trajectories for each new t' in the integral. The CS projection onto the initial state $-\mathcal{E}_0\langle pq\gamma_2|x|\Phi_0\rangle$ can be evaluated analytically and its amplitude was used as the sampling function for the phase space integral. The values of $\gamma_2 = \gamma$ and $\gamma_1 = \gamma/32$ were used for both the HK and the semiclassical strong field S-matrix approximation in this case.

Figure 1(a) shows $|\Psi(t)|$ at $t = 150$ a.u. calculated using a fully quantum simulation, the HK method with 10^6 trajectories, and the SSF approximation with 10^6 trajectories. The quantum wave function (thick line) exhibits a long tunneling portion which is leaking from the core continuously (steady-state tunneling). The hump at the
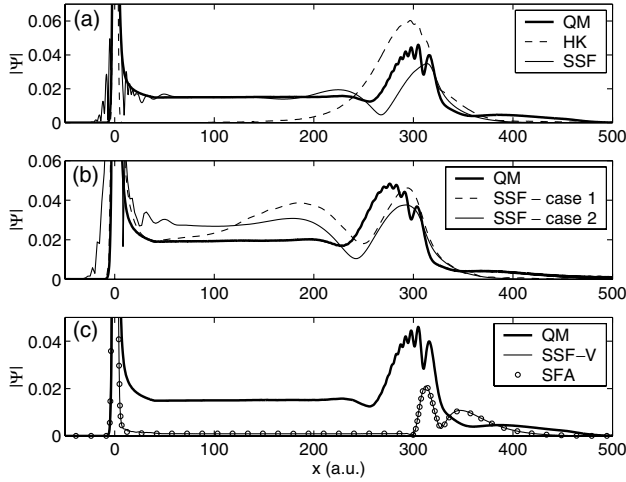
FIG. 1. Results for 1D simulations. (a) Wave function amplitude $|\Psi|$ calculated at $t = 150$ a.u. for the case of $a = 1$: quantum (thick), HK (dashed), and SSF (thin). (b) Wave function at $t = 200$ a.u. for the case of $a = 1.59$: quantum (thick), SSF for parameters $\{\gamma_1 = \gamma, \gamma_2 = \gamma\}$ (dashed) and for $\{\gamma_1 = \gamma/32, \gamma_2 = \gamma\}$ (thin). (c) As (c) using full quantum (thick), SSF with strong field assumption (thin), quantum strong field approximation (open circles).

leading edge of the escaping wave function is due to the above-barrier energy content of the initial state which immediately propagates away from the core.

As anticipated, the results for the HK method (dashed line) show no amplitude in the steady-state tunneling regime. The lack of a long-time steady-state tunneling regime arises because the HK expression has no mechanism of "tunneling out" initially trapped trajectories. The SSF wave function (thin line), however, shows excellent agreement with the steady-state tunneling regime as well as good agreement with the above-barrier regime. As previously mentioned, the tunneling mechanism in the SSF equation is contained in the time integral which allows a classical trajectory to originate near the core with above-barrier energy at any time throughout the entire time range and hence a continuous "leakage" of the wave function is possible.

Figure 1(b) shows results corresponding to an alternate combination of softcore and field parameters ($a = 1.59$ and $\mathcal{E}_0 = 0.04$). This system approximates a one-electron 1D model of Xe with ground state $E_0 = -0.452$ a.u. ($\gamma = 0.125$). The plot shows the full quantum solution along with the SSF results for the two sets of CS parameters $\{\gamma_1 = \gamma, \gamma_2 = \gamma\}$ and $\{\gamma_1 = \gamma/32, \gamma_2 = \gamma\}$ both using 10^6 trajectories. It can be seen from these two SSF calculations that allowing γ_1 and γ_2 to differ can lead to more accurate results: there is an x dependent "hump" in the tunneling portion of the wave function when CS parameters $\gamma_1 = \gamma_2$ are used which is not present in the case where $\gamma_1 \neq \gamma_2$. The agreement seen here between the quantum and SSF results is not as good as in the previous case, however, this last method again does a

much better job than the HK method at simulating the tunnel dynamics which again failed to reproduce the steady-state tunneling portion of the wave function. The cases presented in Figs. 1(a) and 1(b) are characteristic of the level of accuracy achieved with the SSF method when other a and $\mathcal{E}_0$ were used.

An approximation commonly used in strong field physics [4] is to replace the full propagator in Eq. (6) by the Volkov propagator. The Volkov propagator completely ignores the field-free potential and propagates the wave function in the strong field alone $e^{-i\hat{H}(t-t')} \longrightarrow e^{-i\hat{H}_V(t-t')}$ where $\hat{H}_V = \hat{K} + \hat{V}$ and $\hat{K}$ is the kinetic energy operator. This approximation, called the strong field approximation (SFA), treats the strong field exactly and the atomic potential enters the calculation only during the field-free propagation of the wave function. After ionization the atomic potential is considered a negligible perturbation to the continuum dynamics which is dominated by the strong field.

The full quantum solution, the quantum SFA wave function, and the SSF wave function using the Volkov Hamiltonian (10^6 trajectories), for the same case as Fig. 1(a), are plotted in Fig. 1(c). The quantum strong field and semiclassical wave functions are essentially indistinguishable. This is because the SC-IVR propagators are based on an approximation to the full Feynman path integral which is exact for potentials up to second order. The Volkov propagator includes only the field potential which is a linear function and therefore the semiclassical IVR evaluation of the Volkov propagator is exact. The only deviations are near the discontinuity at $x = 40$ a.u. (i.e., where the potential deviates from a linear function) and even these are quite small.

The steady-state tunneling regime seen in the solution using the Volkov propagator, however, is largely underestimated as compared to the full quantum solution as well as to the results of the (SSF) approximation. The SSF method can then be seen as a means of including core effects semiclassically to the Volkov propagator and thereby greatly improving the accuracy of the standard strong field approximation.

Consider now a 2D softcore atom in a static field. The Hamiltonian is

$$H = \frac{1}{2}(p_x^2 + p_y^2) - \frac{1}{\sqrt{x^2 + y^2 + a^2}} - \mathcal{E}_0 x. \qquad (9)$$

The softcore parameter used, $a = 0.93$, again models Xe with ground state energy $E_0 = -0.452$ a.u. The ground state wave function was approximated with a Gaussian $\gamma = 0.15$. The field strength was $\mathcal{E}_0 = 0.045$. The results for this system calculated using quantum, HK, and SSF methods are shown in Fig. 2 which plots $|\Psi(x, y = 0)|$ at $t = 200$ a.u. Both HK and SSF used $\gamma_1 = \gamma_2 = \gamma$. The HK result used 6×10^6 trajectories while the SSF result used 10^6 trajectories.
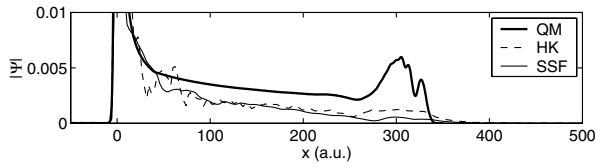
FIG. 2. Results for 2D simulations showing full quantum (QM), Herman-Kluk (HK), and semiclassical strong field S-matrix (SSF) calculations.

Two key points have to be stressed. First, unlike in the 1D case, the HK and the SSF approximate the correct quantum wave function equally well. The fact that the HK method alone reproduces the steady-state tunneling regime is unexpected. In the 1D case, if a particular trajectory has enough energy to make it over the barrier, then it will do so in short time with at most one reflection (if the trajectory had initially negative momentum). All above-barrier trajectories escape at more or less the same time. This leads to the relatively narrow initial burst in the escaping HK wave function as seen in Fig. 1(a). In the 2D case, however, trajectories with above-barrier energy may experience multiple reflections before finally "lining-up" with the suppressed barrier and escaping. Hence, unlike in the 1D case, it is possible in multiple dimensions to have a slow leak of the above-barrier classical trajectories where this gradual leakage is absent in the equivalent 1D system. For larger times, however, the continuous tunneling amplitude will presumably truncate prematurely using the HK method once all the above-barrier trajectories have escaped the core. In this case, the SSF expression would be expected to recover the lost tunneling amplutide again by allowing for new above-barrier trajectories to originate near the core at any moment of time just as in the 1D case.

Second, there is a significant difference in the relative convergence rates of the HK and SSF methods. In 1D, both the HK and SSF calculations were well converged using 10^6 trajectories to perform the Monte Carlo integral. In 2D, the SSF result, which used the same number of trajectories as in 1D (10^6), is reasonably well converged while the HK result, which used 6 times more trajectories, is still far from converging (see Fig. 2).

A rigorous comparison of the relative convergence rates was performed by calculating the fractional statistical error

$$\epsilon(x) = \frac{1}{\langle I(x) \rangle} \sqrt{\frac{\langle I(x)^2 \rangle - \langle I(x) \rangle^2}{N}}, \qquad (10)$$

where $I(x)$ is the semiclassical integrand at point x [or point $\vec{x} = (x, y)$ in 2D] and N is the number of trajectories. For large N, $\epsilon(x)$ becomes simply $\epsilon(x) \sim \sigma_0(x)/\sqrt{N}$ where the constant $\sigma_0(x)$ completely characterizes the asymptotic convergence rate. Table I presents the calcu-

TABLE I. Convergence properties of the HK and the SSF approach for 1D and 2D.

Dim.	σ_0 (HK)	σ_0 (SSF)
1	6.4	15
2	150	74

lated σ_0 [which are averages of $\sigma_0(x)$ over many points along the wave functions, i.e., $\sigma_0 = \sum_i \sigma_0(x_i)$] for the various calculations presented herein. Going from 1D to 2D for the HK method increases σ_0 by a factor of 20 which leads to a factor of $20 \cdot 20 = 400$ increase in the number of required trajectories to achieve a comparable level of convergence. For the SSF method, moving from 1D to 2D leads to only a factor of 5 increase in σ_0 which means a factor of 25 increase in the number of trajectories. Thus, the SSF method exhibits favorable scaling of the convergence rate with increasing dimensionality.

The SSF method has been shown to give good results for the problem of atomic tunnel ionization in a static field and it would certainly be of interest to apply this method to other tunneling problems. However, the SSF method needs to have the full Hamiltonian split into a field-free part $\hat{H}_0$ and a strong perturbing field $\hat{V}$. Although this distinction is obvious in the case of an atomic core in the presence of a strong field, some interesting tunneling problems may not have such a conveniently partitioned Hamiltonian. Double well systems [6], for example, offer interesting tunneling dynamics but have ill-suited Hamiltonians for the formalism presented here. The SSF method in the present form would then be more suitable for studying strong field dynamics, for example, an atom/molecule interacting with a laser field or laser-assisted atom-electron collisions.

[1] S. Keshavamurthy and W. H. Miller, Chem. Phys. Lett. **218**, 189 (1994).
[2] F. Grossmann and E. J. Heller, Chem. Phys. Lett. **241**, 45 (1995); N. T. Maitra and E. J. Heller, Phys. Rev. Lett. **78**, 3035 (1997).
[3] W. H. Miller, J. Phys. Chem. A **105**, 2942 (2001).
[4] H. R. Reiss, Prog. Quantum Electron. **16**, 1 (1992).
[5] F. Grossmann, Phys. Rev. Lett. **85**, 903 (2000).
[6] J. C. Burant and V. S. Batista, J. Chem. Phys. **116**, 2748 (2002).
[7] G. van de Sand and J. M. Rost, Phys. Rev. Lett. **83**, 524 (1999); Phys. Rev. A **62**, 053403 (2000).
[8] M. F. Herman and E. Kluk, Chem. Phys. **91**, 27 (1984).
[9] K. G. Kay, J. Chem. Phys. **100**, 4432 (1994).
[10] T. Brabec and M. Walser (private communication).